

COLLISION EFFICIENCIES OF DIFFUSING SPHERICAL PARTICLES: HYDRODYNAMIC, VAN DER WAALS AND ELECTROSTATIC FORCES

IRAKLIS A. VALIOULIS and E. JOHN LIST

California Institute of Technology, Pasadena, California, USA

CONTENTS

- I. ABSTRACT
- II. INTRODUCTION
- III. HYDRODYNAMIC INTERACTIONS
- IV. VAN DER WAALS FORCES
- V. COLLISION EFFICIENCIES
- VI. DOUBLE LAYER FORCES
- VII. CONCLUSIONS
- VIII. ACKNOWLEDGEMENTS

I. ABSTRACT

A practical limitation of the application of Smoluchowski's classical estimate for the collision probability of two diffusing spherical particles in Brownian motion is the non-consideration of interparticle forces. For suspended particles in water such forces can arise from the disturbance the particle causes in the fluid (hydrodynamic forces), from the cloud of ions which surround an electrically charged particle (double layer forces) or they can be of molecular origin (van der Waals forces). In this paper corrections to Smoluchowski's collision probability are computed when such forces operate between two approaching particles of various sizes. Results for several values of the van der Waals energy of attraction and the ionic strength of the electrolyte are presented in a way convenient for particle collision modeling.

II. INTRODUCTION

Suspended particles are ubiquitous in most environmental or industrial flows. They affect both the bulk properties of the fluid and the surfaces with which the suspension is in contact. Information on the physical characteristics of the individual particles and the properties of the flow is required in order to predict the behavior of the suspension. The knowledge of the fluid-particle

interactions, however, is not sufficient for successful modeling of flows in which particles interact with each other. Coagulation, the process of collision and coalescence of particles, modifies the distribution of suspended mass in the particle size space. Particle-particle interactions thus become important in quantifying the fate of suspended matter in flows in which coagulation occurs.

For particles in the size range $0.1\mu\text{m}$ - $10\mu\text{m}$ Brownian diffusion is the dominant coagulation mechanism (ref. 2). If it is assumed that the suspension is sufficiently dilute so that only binary particle encounters occur, then the collision rate, per unit volume of fluid, of particles with radii r_1 and r_2 is given by the product of their respective number concentrations N_1 and N_2 and a collision function (collision probability) $\beta(r_1, r_2)$, representing the geometry and dynamics of the Brownian process:

$$\text{collision rate} = \beta(r_1, r_2) N_1 N_2 \quad (1)$$

The collision probability $\beta(r_1, r_2)$ is equal to the common volume the two diffusing particles sweep per unit time in a unit volume of fluid. When the particles are much larger than the molecular mean free-path of the fluid the collision function is computed (ref. 3) by solving a diffusion equation for the pair distribution function of the two particles. More specifically, $\beta(r_1, r_2)$ is equal to the asymptotic flux to the surface of a fixed sphere of radius $r_1 + r_2$ with diffusivity $D_1 + D_2$, where D_i is the diffusivity of particle with radius r_i , for $i=1,2$. The pair distribution function is held at zero at the surface of the fixed sphere and unity at infinity. Then for times larger than the particle viscous relaxation time, $t = 2r^2/9\nu$, the collision function is

$$\beta(r_1, r_2) = \frac{2}{3} \frac{kT}{\mu} \frac{(r_1 + r_2)^2}{r_1 r_2} \quad (2)$$

where k is Boltzmann's constant, T is the absolute temperature and μ is the fluid dynamic viscosity.

This expression ignores particle interactions, that is, it assumes that particles move on straight paths. However, as particles approach each other, interparticle forces modify their relative motion. For suspended particles in water such forces can arise from the disturbance the presence of the particle causes in the fluid (hydrodynamic forces), from the cloud of ions which surround an electrically charged particle (double layer forces), or they can be of molecular origin (van der Waals forces). A correction (collision efficiency or collision enhancement) $E(r_1, r_2)$ is then defined which multiplies the 'rectilinear' collision rate (as given by Eqs. 1 and 2) and incorporates the influence

of the interparticle forces on the collision process.

In this paper we extend a method used first by Spielman (ref. 4) for monodisperse suspensions to compute the collision efficiencies of two diffusing spherical particles of various sizes in Stokes' flow accounting for van der Waals and double layer forces. Results over a wide range of values of the Hamaker constant, A , and of the relative size of the particles, r_2/r_1 , are presented in a way convenient for particle collision modeling.

III. HYDRODYNAMIC INTERACTIONS

Smoluchowski's (ref. 1) classical model for Brownian motion induced coagulation applies to extremely dilute systems where only binary particle encounters are considered. The two particles are treated as rigid spheres describing Brownian motions independently of each other with a constant relative diffusion coefficient

$$D_{12} = D_1 + D_2, \quad (3)$$

where the single particle diffusion coefficients

$$D_1 = kTb_1, \quad D_2 = kTb_2 \quad (4)$$

are functions of the particle mobilities b_1 and b_2 which are determined by Stokes' law. For a particle of radius r the mobility is $b = 1/(6\pi\mu r)$. However, this formulation ignores hydrodynamic forces which tend to correlate the particle motions as the particle separation decreases. The motion of one particle generates a velocity gradient of order s^{-2} at distance s in the surrounding fluid. This velocity gradient causes a particle located at that distance to act as a force dipole which induces a velocity of order s^{-4} at the location of the first particle (ref. 5). Thus, Eq. 3 becomes increasingly invalid as the particle separation decreases.

Spielman (ref. 4) modified the relative diffusion coefficient to account for such particle interactions by extending Einstein's (ref. 6) ingenious argument. In an unbounded system of particles a hypothetical dynamic equilibrium is assumed: at any point in space, the mean radial number density flux J_D of particles 2 relative to particle 1 due to Brownian diffusion is balanced by an advective flux J_F . The latter arises from the action of an arbitrary steady conservative force F derivable from a potential V and acting between the particles:

$$J_D + J_F = 0 \quad (5)$$

$$J_D = -D_{12} (dN_2/dr), \quad J_F = N_2 \cdot u \quad (6)$$

where N_2 is the number density of particles 2 and u the relative radial velocity imparted to the particles by the conservative force F

$$u = bF, \quad \text{where } F = -dV/dr. \quad (7)$$

Here b is the relative particle mobility which is a function of separation.

Under equilibrium conditions the number density of particles 2 must be Boltzmann distributed

$$N_2 = N_2^\infty \exp(-V/(kT)), \quad (8)$$

where N_2^∞ is the number density of particles 2 at infinite interparticle distance. Then the relative particle diffusion flux is

$$J_D = -D_{12} (dN_2/dr) = (D_{12}/(kT)) (dV/dr) N_2 \quad (9)$$

and the flux induced by the conservative force F

$$J_F = -N_2 b (dV/dr) \quad (10)$$

The hypothetical equilibrium situation (Eq. 5) is invoked then to deduce from Eqs. 9 and 10 the relative particle diffusivity

$$D_{12} = bkT \quad (11)$$

which is a function of interparticle separation. Following Einstein (ref. 6) it is now assumed that Eq. 11 is valid even when the force F is removed. This is only justified if inertial effects are ignored so that the two fluxes become superposable (ref. 5). The relative mobility b can be computed from the exact solution of Stokes' equations for two spheres moving along their line of centers obtained by Stimson and Jeffery (ref. 7). Both the rotational motion and the motion perpendicular to the line of centers of the particles are irrelevant when spherical particles are considered, since all motions are independent in Stokes' flow (ref. 4).

The hydrodynamic force between two approaching particles determined from the linearised equations of motion becomes singular at zero separation. This unphysical behavior is explained by the breakdown of continuum flow at distances of the order of the fluid molecular mean free path. Van der Waals short range forces which diverge at particle contact can be considered to overcome this

difficulty in the collision problem.

IV. VAN DER WAALS FORCES

The attractive London-van der Waals forces arise from the synchronized dipoles created by fluctuating charges in the electron clouds of the interacting bodies. Hamaker (ref. 8) assumed additivity of the pairwise interactions of the constituent atoms and molecules and derived his well-known formula for the van der Waals interaction energy V_A between spherical particles.

$$\frac{V_A}{kT} = -\frac{A}{6kT} \left[\frac{2r_1r_2}{r^2 - (r_1+r_2)^2} + \frac{2r_1r_2}{r^2 - (r_1-r_2)^2} + \log \frac{r^2 - (r_1+r_2)^2}{r^2 - (r_1-r_2)^2} \right] \quad (12)$$

Here r is the distance between particle centers and A is the Hamaker constant. Schenkel and Kitchener (ref. 9) incorporated retardation effects in Hamaker's formula and recommended the best-fit approximation to their numerical integrations

$$\frac{V_A}{kT} = -\frac{A}{6kT} \frac{r_2}{h(r_1+r_2)} \frac{1}{1+1.77p}, \quad 0 < p < 0.57 \quad (13)$$

$$\frac{V_A}{kT} = -\frac{2A}{kT} \frac{r_2}{h(r_1+r_2)} \left[-\frac{2.43}{60p} + \frac{2.17}{180p^2} - \frac{0.59}{420p^3} \right], \quad p \geq 0.57$$

where $p = 2\pi h/\alpha$ and $\alpha = \lambda/r_1$; h is the dimensionless minimum distance between the particles, $h = (r-r_2-r_1)/r_1$ and $\lambda = 100\text{nm}$ is the London wave length; λ introduces another length in the problem, so the collision efficiencies become a function of the absolute size of the particles.

Electromagnetic retardation occurs when the interparticle distance is larger than the characteristic wavelength of the radiation emitted by the induced dipoles and is due to the finite time of propagation of electromagnetic waves (ref. 10). Since Eq. 13 incorporates only a single characteristic wavelength it can only account qualitatively for the retardation effects. The latter render the Hamaker 'constant', A , a function of the particle separation (ref. 11). Nevertheless, Eq. 13, because of its simple form, has been used (ref. 12) to calculate an 'effective' Hamaker constant from experiments involving a coagulating monodisperse population of particles. Provided then that A is obtained from such an experiment, Eq. 13 may be a good approximation in modeling the kinetics of coagulation in a polydisperse suspension.

The generalized Smoluchowski equation for the diffusing particles under the action of interparticle conservative forces is (ref. 4)

$$\frac{\partial N_2}{\partial t} = -\text{div} J_{12} = \frac{1}{r^2} \frac{\partial}{\partial r} \left[r^2 \left(D_{12} \frac{\partial N_2}{\partial r} + N_2 b \frac{dV_A}{dr} \right) \right], \quad (14)$$

with boundary conditions

$$\begin{aligned} N_2 = 0 \quad \text{and} \quad V_A = -\infty \quad \text{when} \quad r = r_1 + r_2 \\ N_2 = N_2^\infty \quad \text{and} \quad V_A = 0 \quad \text{when} \quad r = \infty \end{aligned} \quad (15)$$

The steady state solution of this equation gives the diffusive flux J_{12} of particles 2 into a sphere of radius $r_1 + r_2$

$$-4\pi r^2 J_{12} = \frac{4\pi D_\infty N_2^\infty (r_1 + r_2)}{\left(1 + \frac{r_2}{r_1}\right) \int_{1+r_2/r_1}^{\infty} \left(\frac{D_\infty}{D_{12}}\right) \exp\left(\frac{V_A}{kT}\right) \frac{ds}{s^2}}, \quad (16)$$

where D_{12} is the relative particle diffusion coefficient in the absence of any interparticle forces and s the dimensionless separation $s = r/r_1$. The collision rate depends on the integral of the particle interactions over all separations. A collision efficiency can be defined

$$E^{-1}(r_1, r_2) = \left(1 + \frac{r_2}{r_1}\right) \int_{1+r_2/r_1}^{\infty} \left(\frac{D_\infty}{D_{12}}\right) \exp\left(\frac{V_A}{kT}\right) \frac{ds}{s^2} \quad (17)$$

as the enhancement of the collision rate over the collision rate in the absence of any interactions between the particles. $E(r_1, r_2)$ is the inverse of Fuchs' (ref. 13) stability factor.

V. COLLISION EFFICIENCIES

The relative diffusion coefficients, D_{12} , were determined as a function of particle separation by summing the series solution to Stokes' equations obtained by Stimson and Jeffery (ref. 7) (as corrected by Spielman, ref. 4). A single convergence criterion $c = 0.0001$ was used for each series, which were assumed to converge when the condition $|(S_{n+1} - S_n)/S_n| < c$ was fulfilled; S_n is the n^{th} -partial sum of a series. All the numerical calculations were performed to a precision of thirteen significant figures. For dimensionless separations $h < 0.001$, the asymptotic formula

$$\frac{D_{12}}{D_\infty} = \left(\frac{r_1}{r_2} + 1\right) h \quad (18)$$

developed by Brenner (ref. 14) was used; this speeds up the calculations since the series converges slowly at small separations.

The integration in Eq. 17 was performed numerically using Simpson's formula. A successively decreasing integration step was used to account for the more rapid variation of the integrand with decreasing particle separation. The integration ranged over a dimensionless separation $10^{-6} < r/r_2 < 500$, where r_2 is the larger of the two particles; extending the integration range did not alter the results.

To assess the significance of retardation, both the unretarded (Eq. 12) and the retarded (Eq. 13) potential were used to compute collision efficiencies for particles of equal size and for various values of $A/(kT)$. Fig. 1 is a comparison between the unretarded and retarded potential for different values of the retardation parameter α . The curves collapse for dimensionless separations s less than about 0.001; for larger interparticle distances electromagnetic retardation reduces the attractive potential significantly. The curve for the retarded potential in Fig. 1 approaches the curve for the unretarded potential as r_1 decreases (or as α increases); the limit $\alpha \rightarrow \infty$ corresponds to the unretarded case.

In the calculations represented by the curves marked with W in Fig. 2 hydrodynamic interactions are ignored; the curves marked with H represent collision efficiencies when both van der Waals and hydrodynamic forces operate. Retardation assumes increasing importance as the van der Waals energy of attraction increases. The hydrodynamic forces tend to dominate the collision process as the van der Waals forces become of shorter range.

The efficiencies computed with the unretarded potential for equal size particles agreed very well with Spielman's results; this provided a check for the validity of the calculations.

The effect of the relative size of the interacting particles on the collision efficiency when only van der Waals forces are considered is shown in Figs. 3 and 4 for $\alpha = 0.1$ and $\alpha = 1$, respectively (with $\lambda = 100\text{nm}$, $\alpha = 0.1$ corresponds to a particle radius $r_1 = 1\mu\text{m}$ and $\alpha = 1$ corresponds to $r_1 = 0.1\mu\text{m}$). The enhancement of the collision rate decreases as both the absolute and the relative size of the interacting particles decrease. The computed efficiencies are lower than the ones calculated by Twomey (ref. 15), who did not include retardation, and are in agreement with the results obtained by Schmidt-Ott and Burtscher (ref. 16).

Hydrodynamic forces reduce the collision efficiency of interacting particles (Figs. 5, 6 and 7). For large particles ($r_1 = 1\mu\text{m}$ or $\alpha = 0.1$) at all values of $A/(kT)$ examined and for smaller particles at $A/(kT)$ less than about 20, the collision efficiency is reduced more between particles of similar size. This effect is illustrated in Fig. 7 where the reduction in the collision efficiency due to hydrodynamic forces for different particle pairs and at various values

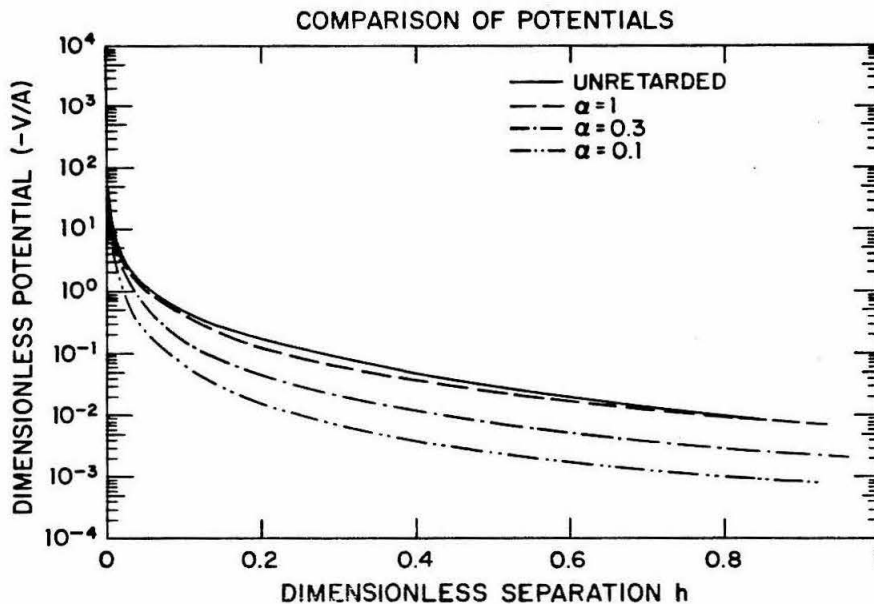


Fig. 1. Dimensionless van der Waals potential vs. dimensionless particle separation for various values of the retardation parameter α .

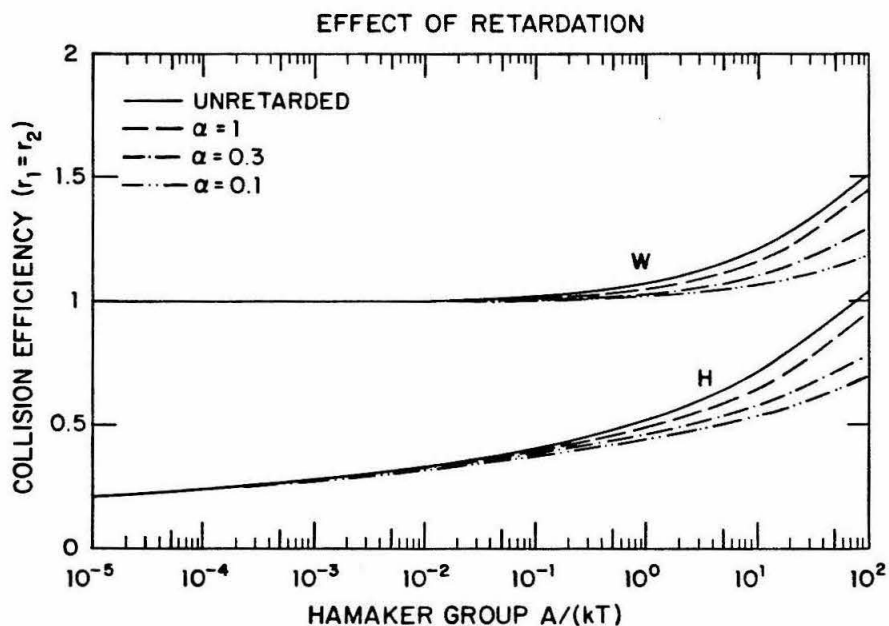


Fig. 2. Effect of retardation on the collision efficiency of equal size particles for various values of $A/(kT)$.

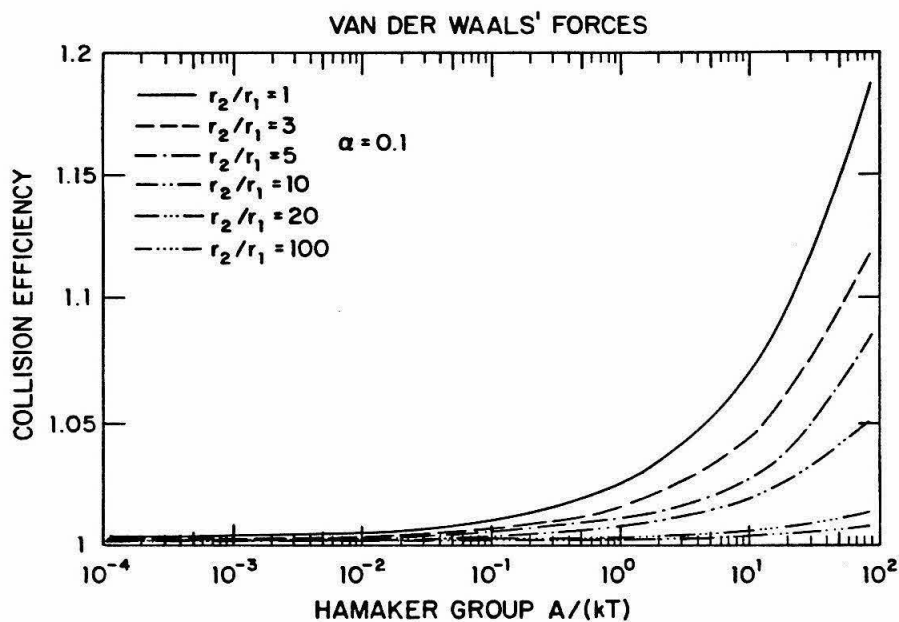


Fig. 3. Collision efficiencies of particles with various relative sizes and for various values of $A/(kT)$ when only van der Waals forces operate ($\alpha = 0.1$).

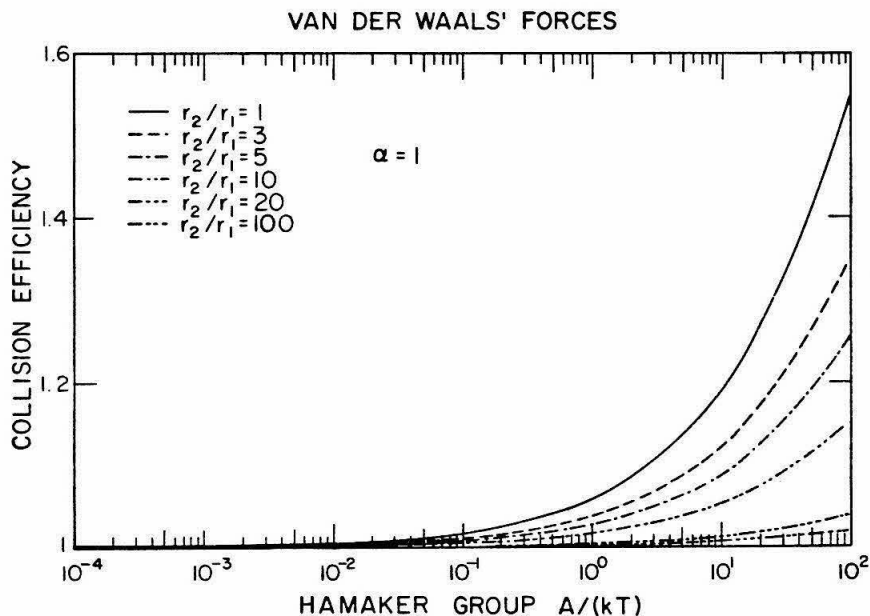


Fig. 4. Collision efficiencies of particles with various relative sizes and for various values of $A/(kT)$ when only van der Waals forces operate ($\alpha = 1$).

of $A/(kT)$ is shown. E_H stands for the collision efficiency when both hydrodynamic and van der Waals forces operate; E_W is the collision efficiency when

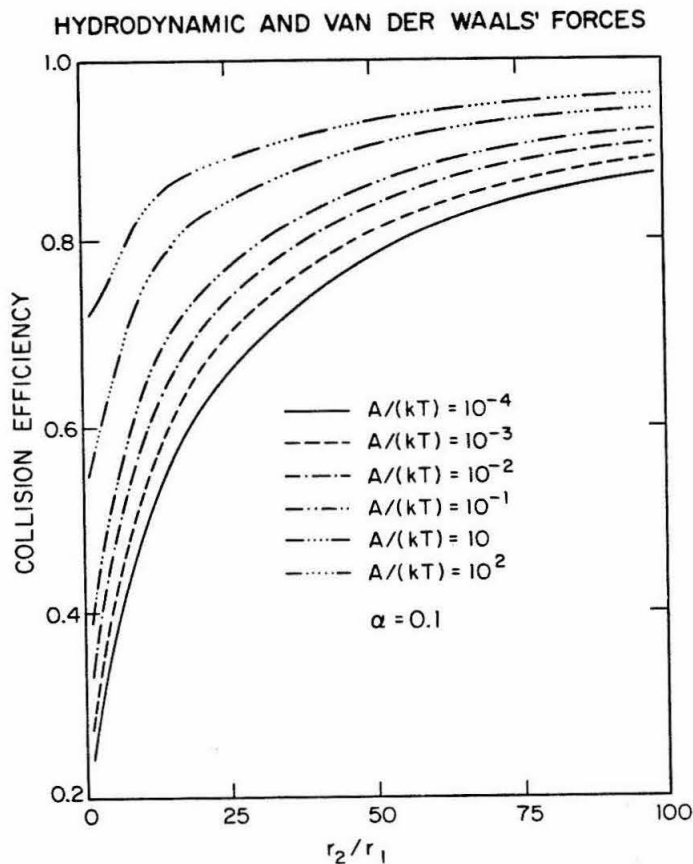


Fig. 5. Collision efficiencies of particles with various relative sizes and for various values of $A/(kT)$ when van der Waals and hydrodynamic forces operate ($\alpha = 0.1$).

only van der Waals forces act. The curves shown approach zero as the interparticle attractive energy decreases. In the limit $A \rightarrow 0$ collisions are theoretically impossible since in Stokes' flow the hydrodynamic repulsive force between the particles grows without bound as the particle separation decreases.

For small particles ($r_1 = 0.1 \mu\text{m}$ or $\alpha = 1$) of equal size at large values of $A/(kT)$ the effect of the van der Waals forces on the collision efficiency is particularly strong (see Fig. 4). This reverses the trend toward smaller efficiencies as the ratio r_2/r_1 (where $r_2 > r_1$) decreases caused by the action of the hydrodynamic interparticle force. Witness the upper two curves in Fig. 6: the collision efficiency of equal particles is very large compared with the rest of the curve.

Reported experimental collision efficiencies range from 0.35 to 0.7 for equal size particles in the size range $0.1 \mu\text{m}$ to $1 \mu\text{m}$ (see ref. 12 for a recent

survey), a result which according to Fig. 5 implies a maximum value for the Hamaker constant of about $2 \cdot 10^{-19}$ Joules (at 300°K) for the retarded potential.

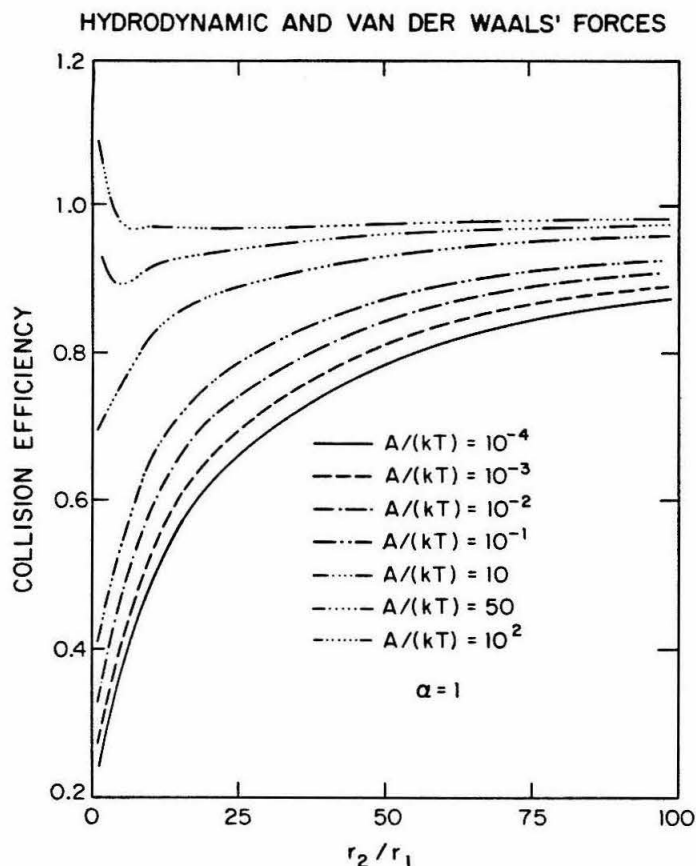


Fig. 6. Collision efficiencies of particles with various relative size and for various values of $A/(kT)$ when van der Waals and hydrodynamic forces operate ($\alpha = 1$).

According to Lyklema (ref. 17), the Hamaker constant of most hydrophobic colloids in water ranges from about 10^{-19} Joules to about $2 \cdot 10^{-22}$ Joules corresponding to Hamaker groups (at 300°K) of about 25 and 0.06, respectively. According to Fig. 5, these correspond to a collision efficiency of about 0.75 and 0.35, respectively (for the retarded potential), which are in the range of collision efficiencies determined experimentally.

Estimation of the Hamaker constant A can be carried out by Lifshitz's (ref. 18) method. This requires knowledge of the frequency ω dependent dielectric permittivities $\epsilon(\omega)$ of the particles and the dispersive medium. However, incomplete information on the function $\epsilon(\omega)$ and the not well known effect of the ionic species in solution on the electromagnetic radiation (ref. 19) complicates the determination of A from dielectric data and suggests that its indirect experimental measurement may be more promising for practical applications. Experimental determination of the Hamaker constant can be carried out

indirectly from the kinetics of coagulation, from data on surface tension and wetting, adsorption, adhesion and the kinetics of film thinning (ref. 19). In

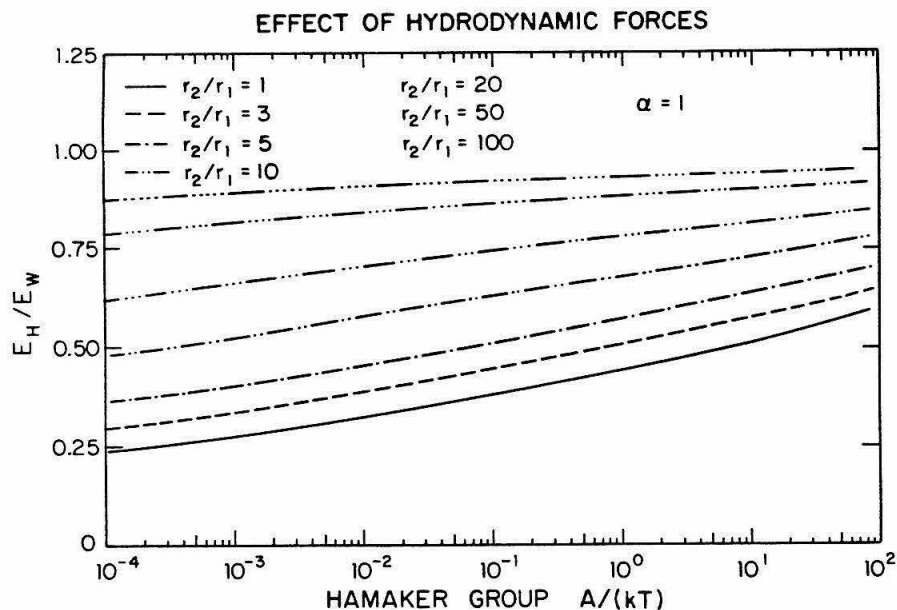


Fig. 7. Evaluation of the relative importance of hydrodynamic and van der Waals forces in modifying the collision rate of two spherical particles.

rapid coagulation experiments of monodisperse systems it is assumed that double layer forces are negligible and the coagulation rate is determined by means of the half-life of the dispersion (ref. 12). A collision efficiency is determined and then numerical calculations (or Figs. 5 and 6) can give a reasonably reliable value of the Hamaker constant. Modeling of the coagulation process in a polydisperse suspension via the General Dynamic Equation (ref. 20) can be accomplished then, since the collision efficiencies between particles of unlike sizes can be obtained readily from Fig. 5 or Fig. 6.

VI. DOUBLE LAYER FORCES

Dispersed particles in natural waters carry an electric charge. Since the dispersion is electrically neutral, the aqueous phase carries an equal charge of opposite sign. Close to the particle surface a compact layer of specifically adsorbed ions is formed (Stern layer). The outer (Gouy) layer consists of the excess of oppositely charged ions (counter ions) of the dispersing medium. According to the Gouy-Chapman model (ref. 21) an equilibrium is established in the outer (diffuse) layer between electrostatic forces and forces due to the thermal motion of the ions. This causes the diffuse layer to extend outwards from the particle surface into the solution, the concentration of counter ions diminishing with distance.

This local distribution of charges in an electrically neutral solution induces double layer interaction forces between approaching particles. Significant simplifications are needed in order to describe quantitatively the

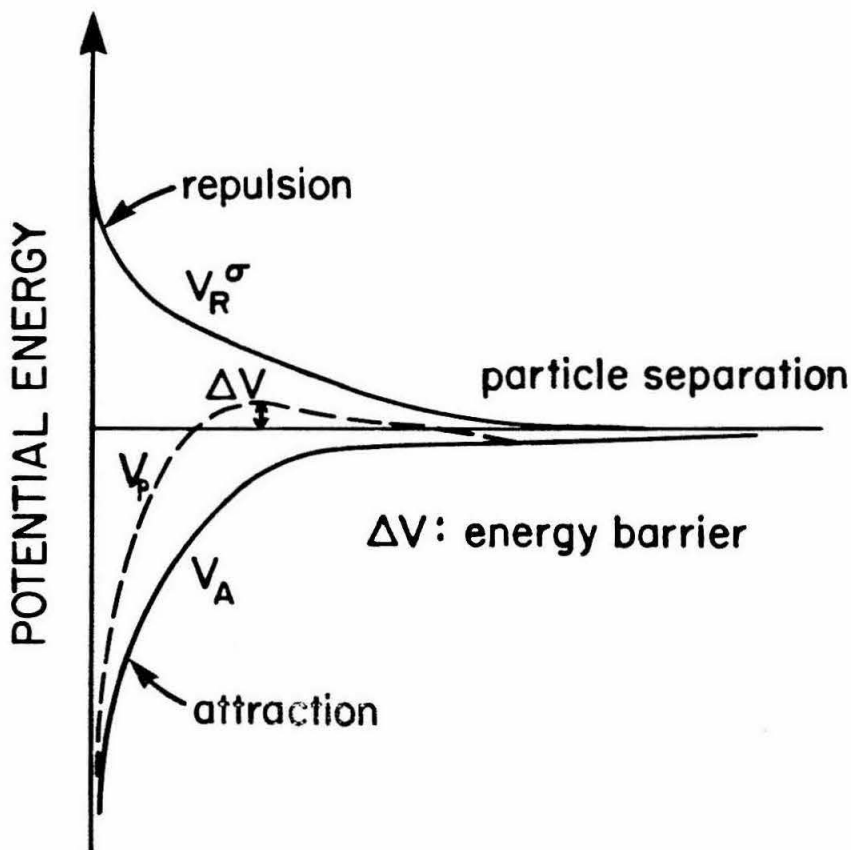


Fig. 8. Schematic illustration of the potential energy as a function of particle surface separation.

interparticle double layer forces. A sufficiently dilute system of negatively charged spherical particles is assumed so that only binary particle encounters are considered. The particles can have different sizes but carry the same charge. In most natural waters suspended particles in the size range $0.1\mu\text{m}$ to $10\mu\text{m}$ have a thin double layer compared with their size (ref. 22). Lyklema and Van Leeuwen (ref. 23) compared the time scale of the Brownian interaction of two colloidal particles with the time scale for the restoration of electrochemical equilibrium on the surfaces of the particles. Their analysis suggests that for double layers which are thin compared with the size of the particles the surface charge density rather than the surface potential remains constant during the time scale of the Brownian interaction. Valioulis (ref. 24) outlined a method to compute the electrostatic potential between two spherical particles carrying the same negative charge. His expressions are lengthy and will not be presented here. He invokes the linear superposition approximation to the diffuse layer interaction between spheres obtained by Bell et al.

(ref. 25) for large interparticle distances. For small separations Derjaguin's (ref. 26) approximation is used.

The collision efficiency of spherical particles subject to Brownian diffusion and accounting for hydrodynamic, van der Waals and double layer forces can be computed from Eq. 17 where now the interaction energy of the two approaching particles is the sum* of the attractive van der Waals potential V_A and the repulsive electrostatic potential V_R^σ at constant surface charge

$$V = V_A + V_R^\sigma \quad (19)$$

The salient features of the curve of the interaction energy V against separation are shown in Fig. 8. At small and large particle separations the van der Waals energy outweighs the repulsion. At intermediate separations the electrostatic repulsion predominates creating a maximum in the potential energy curve (energy barrier). This energy barrier reduces the coagulation rate between two particles and can even prevent them from colliding. Since the collision efficiency (Eq. 17) involves V as an exponential factor the height of the energy barrier is the most significant factor governing the behavior of the collision efficiency; the rest of the curve in Fig. 8 is of little importance.

Fig. 9 shows the effect of the van der Waals energy of attraction on the collision efficiency of the interacting pairs. The ionic strength $I = 0.05$ and both particles have the same (negative) dimensionless undisturbed surface potential $\psi = 0.5$, corresponding to a surface charge density $\sigma = 0.67 \cdot 10^{-6} \text{Cb/cm}^2$. The sequence of Figs. 9, 10 and 11 illustrate the effect of the ionic strength on the collision efficiency. For the range of $A/(6kT)$ in which the efficiency is non-zero the curves overlap. This is the regime of 'rapid' coagulation where the particle behavior is not influenced by electrostatic interactions. The transition from kinetically stable (no significant change in the number density of the particles during the observation time) to unstable state of the dispersion shifts to smaller $A/(6kT)$ as the ionic strength of the solution increases. The transition is abrupt, so a quantitative criterion of coagulation (or stability) can exist.

For the computations presented the unretarded potential (Eq. 12) is used. Practically there is no change in the transition from slow to rapid coagulation when the retarded potential (Eq. 13) is used. This agreement occurs because the energy barrier for coagulation is typically at a dimensionless particle separation, $\kappa \cdot r$ (where κ^{-1} is the double layer thickness), of order 1 where

*There is no firm basis for the superposition of the van der Waals and the double layer force. The interrelation of the two forces, however, is not well understood (see discussion in ref. 19, p. 54).

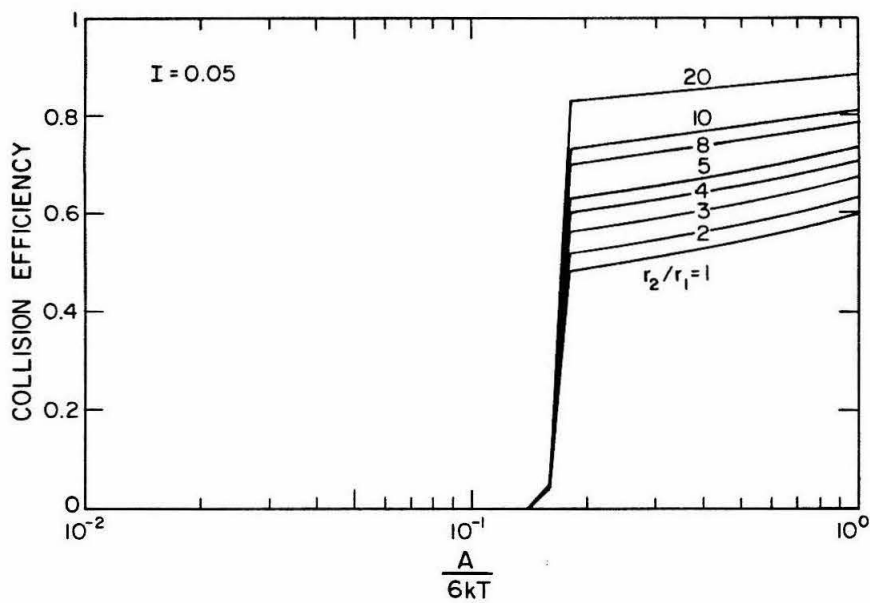


Fig. 9. Collision efficiencies of particles in Brownian diffusion ($I = 0.05$).

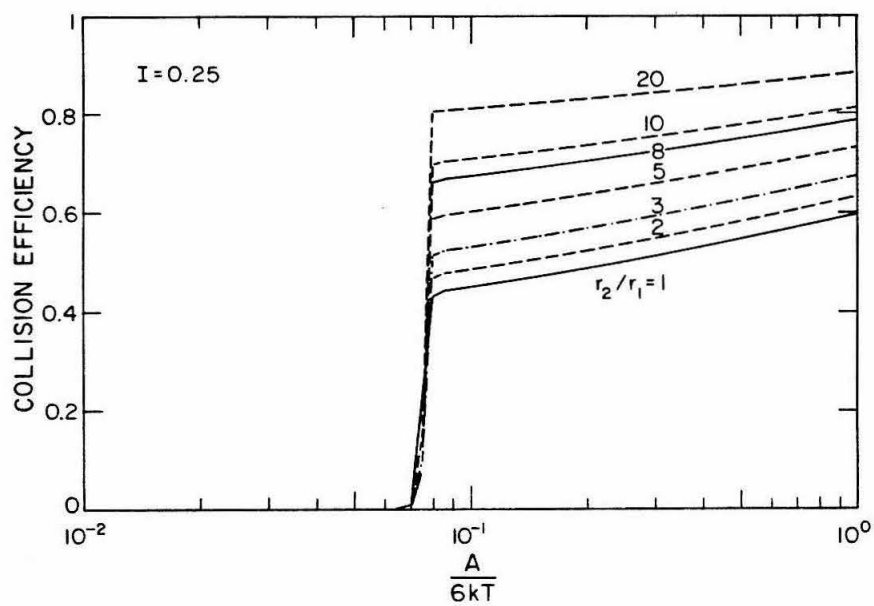


Fig. 10. Collision efficiencies of particles in Brownian diffusion ($I = 0.25$).

retardation effects are not important.

The rapid variation of the collision efficiency with the van der Waals energy of attraction occurs in the 'slow' coagulation regime. According to

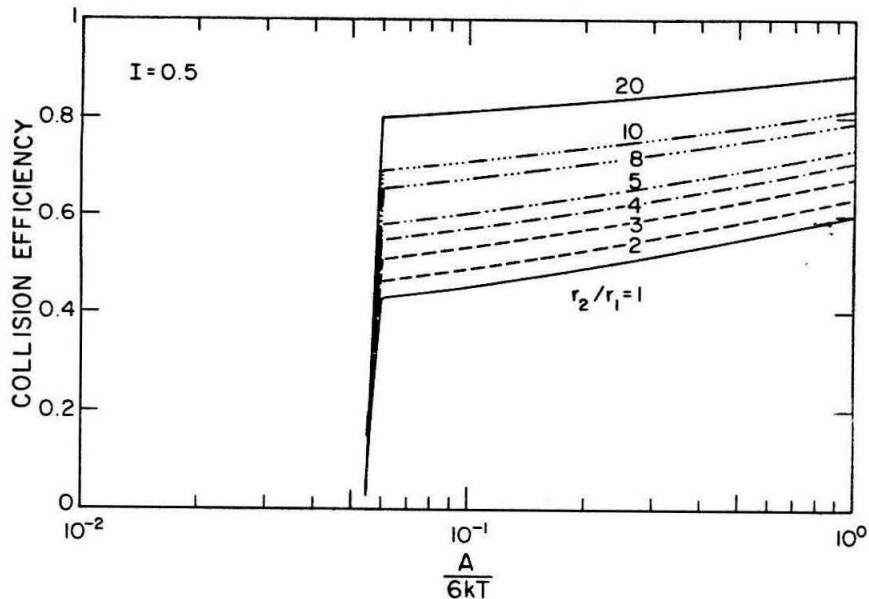


Fig. 11. Collision efficiencies of particles in Brownian diffusion ($I = 0.5$).

Figs. 9, 10 and 11 the transition from slow to rapid coagulation is independent of particle size. This is consistent with experimental results (ref. 27) and theoretical calculations (ref. 28). Collision efficiencies are very small here, so the dispersion is stable for the time scales of most practical applications. The half-life time $t_{1/2}^S$ in which the number N of particles in an initially monodisperse system is reduced to one-half the original value by Brownian motion is (ref. 1)

$$t_{1/2}^S = \frac{3\mu}{4kTN} \quad (20)$$

Here any particle interactions are ignored. (Eq. 20 is approximate since only collisions between primary particles of radius r are considered). The collision efficiency as defined in Eq. 17 is equivalent to

$$E(r_1, r_2) = \frac{t_{1/2}^S}{t_{1/2}} \quad (21)$$

where in $t_{1/2}$ hydrodynamic, van der Waals and electrostatic interactions between the particles are considered. For water at ambient temperature (20°C) Eq. 21 reduces to (ref. 21)

$$t_{1/2} = E(r_1, r_2) \frac{2 \cdot 10^{11}}{N} \quad (22)$$

where N is the number of particles per cm^3 and $t_{1/2}$ is in seconds.

The number of particles in primary sewage sludge is, for example, of order 10^9 cm^{-3} corresponding to a half-life time of $t_{1/2} = E \cdot 55$ hrs. Natural waters have particle number densities of order $10^5 - 10^7 \text{ cm}^{-3}$ (ref. 29). A collision efficiency smaller than 0.001 implies a stable dispersion for all practical purposes. Consequently, only the transition from slow to rapid coagulation, given by the bend in the curves in Figs. 9, 10 and 11 is of interest. Honig and Mull (ref. 30) ignored hydrodynamic interactions and computed the critical electrolyte concentration at the onset of coagulation in a monodisperse system of particles with constant charge surfaces. Their criterion for the onset of rapid coagulation is a function of the ionic strength of the electrolyte, the particle surface charge and the van der Waals energy of attraction. Their analysis is equally valid for polydisperse systems and when hydrodynamic interactions occur between particles (ref. 24) and thus it can be used to evaluate the stability of a polydisperse population of particles for any combination of I , σ and A .

VII. CONCLUSIONS

The aim of the work described in this paper has been to improve the collision rate given by Smoluchowski's (ref. 1) classical theory for Brownian diffusion. The computed collision efficiencies take into account hydrodynamic, van der Waals and double layer interactions between two approaching particles.

The short-range van der Waals potential and the long-range hydrodynamic forces tend to affect both the collision rate and the functional dependence of the collision rate on the relative sizes of the interacting particles. For practical applications (wastewater treatment, water purification, prediction of sediment concentration in ocean discharges) only rapid coagulation is important. Double layer forces determine the onset of coagulation. Once collisions occur, the coagulation rate is determined solely from the relative mobility of the particles (modified to account for hydrodynamic forces) and the Hamaker constant. The onset of coagulation is abrupt, so a quantitative criterion of stability can exist.

From well-controlled experiments with an initially monodisperse suspension of coagulating particles an 'effective' Hamaker constant can be determined. From the results of the calculations presented here the collision efficiencies of particles of unlike sizes can be estimated. Tables 1 and 2 and Figs. 5 and 6 serve this purpose. The curves in Figs. 5 and 6 are given in parametric form in Table 3. Interpolation can be used for intermediate values of the Hamaker

constant. The function $E(r_1, r_2)$ is thus obtained for all pairs of particle sizes, (r_1, r_2) , of interest and so it can be incorporated into the General Dynamic Equation to obtain realistic results in modeling of physical processes which involve coagulating particles, (ref. 31).

TABLE 1

Collision efficiencies for Brownian diffusion; retardation parameter $\alpha = 0.1$

van der Waals forces

r_2/r_1	1	3	5	10	20	50	100
$A/(kT)$							
10^{-4}	1.0040	1.0027	1.0024	1.0022	1.0021	1.0021	1.0020
10^{-3}	1.0042	1.0028	1.0028	1.0023	1.0022	1.0021	1.0020
10^{-2}	1.0053	1.0035	1.0030	1.0025	1.0023	1.0021	1.0020
10^{-1}	1.0098	1.0064	1.0040	1.0037	1.0029	1.0024	1.0022
10^0	1.0248	1.0157	1.0116	1.0075	1.0049	1.0032	1.0026
10	1.0691	1.0435	1.0251	1.0189	1.0120	1.0049	1.0040
10^2	1.1983	1.1255	1.0905	1.0540	1.0300	1.0142	1.0082

van der Waals and hydrodynamic forces

r_2/r_1	1	3	5	10	20	50	100
$A/(kT)$							
10^{-4}	0.2409	0.2971	0.3615	0.4810	0.6198	0.7875	0.8763
10^{-3}	0.2791	0.3401	0.4079	0.5287	0.6620	0.8154	0.8936
10^{-2}	0.3286	0.3931	0.4628	0.5824	0.7060	0.8425	0.9101
10^{-1}	0.3867	0.4512	0.5207	0.6338	0.7468	0.8659	0.9237
10^0	0.4546	0.5150	0.5806	0.6841	0.7838	0.8862	0.9354
10	0.5477	0.5981	0.6562	0.7430	0.8245	0.9070	0.9471
10^2	0.7194	0.7335	0.7700	0.8266	0.8796	0.9341	0.9620

TABLE 2

Collision efficiencies for Brownian diffusion; retardation parameter $\alpha = 1$

van der Waals forces

r_2/r_1	1	3	5	10	20	50	100
$A/(kT)$							
10^{-4}	1.0041	1.0027	1.0024	1.0022	1.0021	1.0011	1.0011
10^{-3}	1.0043	1.0029	1.0026	1.0023	1.0021	1.0011	1.0011
10^{-2}	1.0061	1.0041	1.0035	1.0028	1.0024	1.0012	1.0011
10^{-1}	1.0159	1.0108	1.0083	1.0056	1.0040	1.0019	1.0015
10^0	1.0568	1.0375	1.0275	1.0169	1.0101	1.0045	1.0028
10	1.1866	1.1198	1.0868	1.0520	1.0296	1.0127	1.0071
10^2	1.5546	1.3547	1.2572	1.1537	1.0866	1.0379	1.0201

van der Waals and hydrodynamic forces

r_2/r_1	1	3	5	10	20	50	100
$A/(kT)$							
10^{-4}	0.2410	0.2996	0.3647	0.4862	0.6276	0.7867	0.8754
10^{-3}	0.2797	0.3411	0.4090	0.5298	0.6630	0.8152	0.8931
10^{-2}	0.3331	0.3992	0.4694	0.5879	0.7112	0.8441	0.9109
10^{-1}	0.4078	0.4755	0.5450	0.6553	0.7632	0.8740	0.9281
10^0	0.5181	0.5775	0.6384	0.7302	0.8161	0.9019	0.9437
10	0.7025	0.7236	0.7625	0.8217	0.8765	0.9316	0.9603
10^2	1.0955	1.0019	0.9818	0.9682	0.9670	0.9760	0.9844

TABLE 3

Approximations for collision efficiencies in Brownian diffusion accounting for hydrodynamic and van der Waals forces (valid for $1 < r_2/r_1 < 100$)

$$E(r_1, r_2) = a + bx + cx^2 + dx^3, \quad x = r_2/r_1$$

Retardation parameter $\alpha = 0.1$

A/(kT)	a	b x 10 ⁻²	c x 10 ⁻⁴	d x 10 ⁻⁶
10 ⁻⁴	0.21811	2.9593	-4.9962	2.6953
10 ⁻³	0.25878	3.0338	-5.3031	2.9043
10 ⁻²	0.31151	3.0339	-5.4760	3.0409
10 ⁻¹	0.37254	2.9251	-5.4055	3.0318
1	0.44285	2.6954	-5.0576	2.8550
10	0.53814	2.2834	-4.3310	2.4569
10 ²	0.70480	1.3481	-2.4753	1.3845

Retardation parameter $\alpha = 1$

A/(kT)	a	b x 10 ⁻²	c x 10 ⁻⁴	d x 10 ⁻⁶
10 ⁻⁴	0.21770	3.0439	-5.2527	2.8666
10 ⁻³	0.25950	3.0405	-5.3293	2.9227
10 ⁻²	0.31685	3.0423	-5.5222	3.0742
10 ⁻¹	0.39643	2.8985	-5.4343	3.0677
1	0.51062	2.4525	-4.6867	2.6676
10	*0.69014	1.4595	-2.7279	1.5387
10 ²	*0.88418	0.34764	-0.5300	2.7377 x 10 ³

*valid for $2 < r_2/r_1 < 100$

VIII. ACKNOWLEDGEMENTS

The authors gratefully acknowledge the financial support of the Ocean Assessment Division - National Ocean Service - NOAA through Grant No. NA82RAD00004 and the Mellon Foundation through a grant to the Environmental Quality Laboratory at Caltech.

REFERENCES

- 1 M. Smoluchowski, Physik Z., 17(1916)557.
- 2 J.R. Hunt, Report No. AC-5-80, W.M. Keck Laboratory, California Institute of Technology, Pasadena, California, 1980.
- 3 J. Chandrasekhar, Rev. Mod. Phys., 15(1943)1.
- 4 A.L. Spielman, J. Colloid Interface Sci., 33(1970)562.
- 5 G.K. Batchelor, J. Fluid Mech., 74(1976)1.
- 6 A. Einstein, The Theory of the Brownian Movement, Dover, New York, 1926.
- 7 M. Stimson and G.B. Jeffrey, Proc. Roy. Soc. London Ser. A, 111(1926)110.
- 8 H.C. Hamaker, Physica, 4(1937)1058.
- 9 J.H. Schenkel and J.A. Kitchener, Trans. Faraday Soc., 56(1960)161.
- 10 H.B.G. Casimir and D. Polder, Phys. Rev., 73(1948)360.
- 11 J. Mahanty and B.W. Ninham, Dispersion Forces, Academic Press, New York, 1976.
- 12 G.R. Zeichner and W.R. Schowalter, J. Colloid Interface Sci., 71(1979)237.
- 13 N.A. Fuchs, The Mechanics of Aerosols, Pergamon Press, New York, 1964.
- 14 H. Brenner, Advan. Chem. Eng., 6(1966)328.
- 15 S. Twomey, Atmospheric Aerosols, Elsevier, Amsterdam/New York, 1977.
- 16 A. Schmidt-Ott and H. Burtscher, J. Colloid Interface Sci., 89(1982)353.
- 17 J. Lyklema, Advan. Colloid Sci., 2(1968)84.
- 18 E.M. Lifshitz, Sov. Phys. JETP, 2(1956)73.
- 19 B. Vincent and S.G. Whittington, in E. Matijevic (Ed.), Surface and Colloid Science, Plenum Press, New York, 1982.

- 20 F. Gelbard, Y. Tambour and J.H. Seinfeld, *J. Colloid Interface Sci.*, 76(1980)541.
- 21 E.J.W. Verwey and J.T.G. Overbeek, *Theory of the Stability of Lyophobic Colloids*, Elsevier, Amsterdam, 1948.
- 22 W. Stumm and J.J. Morgan, *Aquatic Chemistry*, Wiley-Interscience, 1981.
- 23 J. Lyklema and H.P. Van Leeuwen, *Adv. Colloid Interface Sci.*, 16(1982)227.
- 24 I.A. Valioulis, Ph.D. Thesis, California Institute of Technology, Pasadena, California, 1983.
- 25 G.M. Bell, S. Levine and L.N. McCartney, *J. Colloid Interface Sci.*, 33(1970)335.
- 26 B.V. Derjaguin, *Discuss. Faraday Soc.*, 18(1954)85.
- 27 R.H. Ottewill and J.N. Show, *Disc. Faraday Soc.*, 42(1966)154.
- 28 E.P. Honig, G.J. Roeberson and D.H. Wiersema, *J. Colloid Interface Sci.*, 36(1971)97.
- 29 C.R. O'Melia, *Environ. Sci. Tech.*, 14, 9(1980)1052.
- 30 E.P. Honig and P.M. Mull, *J. Colloid Interface Sci.*, 36(1971)258.
- 31 I.A. Valioulis and E.J. List, *Environ. Sci. Tech.* (in press).